Protective effects of 4-aminopyridine in experimental optic neuritis and multiple sclerosis

Journal Article

Author(s):
Dietrich, Michael; Koska, Valeria; Hecker, Christina; Göttle, Peter; Hilla, Alexander M.; Heskamp, Annemarie; Lepka, Klaudia; Issberner, Andrea; Hallenberger, Angelika; Baksmeier, Christine; Steckel, Julia; Balk, Lisanne; Knier, Benjamin; Korn, Thomas; Havla, Joachim; Martínez-Lapiscina, Elena H.; Sola-Valls, Nuria; Manogaran, Praveena ⓘD; Olbert, Elisabeth D.; Schippling, Sven; Cruz-Herranz, Andrés; Yiu, Hao; Gonzalez Caldito, Natalia; von Gall, Charlotte; Mausberg, Anne K.; Stettner, Mark; Zimmermann, Hannah G.; Paul, Friedemann; Brandt, Alexander U.; Küry, Patrick; Goebels, Norbert; Aktas, Orhan; Berndt, Carsten; Saidha, Shiv; Green, Ari J.; Calabresi, Peter A.; Fischer, Dietmar; Hartung, Hans-Peter; Albrecht, Philipp

BRAIN
A JOURNAL OF NEUROLOGY

Protective effects of 4-aminopyridine in experimental optic neuritis and multiple sclerosis

Michael Dietrich,[1] Valeria Koska,[1] Christina Hecker,[1] Peter Göttle,[1] Alexander M. Hilla,[2] Annemarie Heskamp,[2] Klaudia Lepka,[1] Andrea Issberner,[1] Angelika Hallenberger,[3] Christine Baksmeier,[1] Julia Steckel,[1] Lisanne Balk,[4] Benjamin Knier,[5] Thomas Korn,[5,6] Joachim Havla,[7,8] Elena H. Martínez-Lapiscina,[9] Nuria Solà-Valls,[9] Praveena Manogaran,[10,11] Elisabeth D. Olbert,[10] Sven Schippling,[10,12] Andrés Cruz-Herranz,[13] Hao Yiu,[13] Julia Button,[14] Natalia Gonzalez Caldito,[14] Charlotte von Gall,[3] Anne K. Mausberg,[15] Mark Stettner,[15] Hannah G. Zimmermann,[16] Friedemann Paul,[16] Alexander U. Brandt,[16,17] Patrick Küry,[1] Norbert Goebels,[1] Orhan Aktas,[1] Carsten Berndt,[1] Shiv Saidha,[14] Ari J. Green,[13,18] Peter A. Calabresi,[14] Dietmar Fischer,[2] Hans-Peter Hartung[1] and (iD)Philipp Albrecht[1]

Chronic disability in multiple sclerosis is linked to neuroaxonal degeneration. 4-aminopyridine (4-AP) is used and licensed as a symptomatic treatment to ameliorate ambulatory disability in multiple sclerosis. The presumed mode of action is via blockade of axonal voltage gated potassium channels, thereby enhancing conduction in demyelinated axons. In this study, we provide evidence that in addition to those symptomatic effects, 4-AP can prevent neuroaxonal loss in the CNS. Using *in vivo* optical coherence tomography imaging, visual function testing and histologic assessment, we observed a reduction in retinal neurodegeneration with 4-AP in models of experimental optic neuritis and optic nerve crush. These effects were not related to an anti-inflammatory mode of action or a direct impact on retinal ganglion cells. Rather, histology and *in vitro* experiments indicated 4-AP stabilization of myelin and oligodendrocyte precursor cells associated with increased nuclear translocation of the nuclear factor of activated T cells. In experimental optic neuritis, 4-AP potentiated the effects of immunomodulatory treatment with fingolimod. As extended release 4-AP is already licensed for symptomatic multiple sclerosis treatment, we performed a retrospective, multicentre optical coherence tomography study to longitudinally compare retinal neurodegeneration between 52 patients on continuous 4-AP therapy and 51 matched controls. In line with the experimental data, during concurrent 4-AP therapy, degeneration of the macular retinal nerve fibre layer was reduced over 2 years. These results indicate disease-modifying effects of 4-AP beyond symptomatic therapy and provide support for the design of a prospective clinical study using visual function and retinal structure as outcome parameters.

1 Department of Neurology, Medical Faculty, Heinrich-Heine University Düsseldorf, Düsseldorf, Germany
2 Department of Cell Physiology, Faculty of Biology and Biotechnology, Ruhr-University Bochum, Bochum, Germany
3 Institute of Anatomy II, Medical Faculty, Heinrich Heine University Düsseldorf, Germany
4 Department of Neurology, Amsterdam Neuroscience, MS Center Amsterdam, VU University Medical Center, Amsterdam, The Netherlands
5 Department of Experimental Neuroimmunology, Technische Universität München, Munich, Germany
6 Munich Cluster for Systems Neurology (SyNergy), Munich, Germany
7 Institute of Clinical Neuroimmunology, Ludwig-Maximilians University, Munich, Germany
8 Data Integration for Future Medicine consortium (DIFUTURE), Ludwig-Maximilians University, Munich, Germany

9   Service of Neurology, Hospital Clinic, University of Barcelona, Spain Neuroimmunology Program, Institut d'Investigació Biomèdica August Pi i Sunyer (IDIBAPS), Barcelona, Spain
10 Neuroimmunology and Multiple Sclerosis Research, Department of Neurology, University Hospital Zürich and University of Zürich, Zurich, Switzerland
11 Department of Information Technology and Electrical Engineering, Swiss Federal Institute of Technology, Zurich, Switzerland
12 Neuroscience Center Zurich, University of Zurich and Federal Institute of Technology (ETH) Zurich, Zurich, Switzerland
13 Division of Neuroinflammation and Glial Biology, Department of Neurology, University of California San Francisco, San Francisco, USA
14 Division of Neuroimmunology and Neurological Infections, Johns Hopkins Hospital, Baltimore, USA
15 Department of Neurology, University Hospital Essen, Essen, Germany
16 NeuroCure Clinical Research Center and Experimental and Clinical Research Center, Charité - Universitätsmedizin Berlin, corporate member of Freie Universität Berlin, Humboldt-Universität zu Berlin, and Berlin Institute of Health and Max Delbrueck Center for Molecular Medicine, Berlin, Germany
17 Department of Neurology, University of California, Irvine, USA
18 Department of Ophthalmology, University of California San Francisco, San Francisco, USA

Correspondence to: Philipp Albrecht, MD
Heinrich Heine University Düsseldorf, Moorenstr. 5, 40225 Düsseldorf, Germany
E-mail: phil.albrecht@gmail.com

Introduction

4-Aminopyridine (4-AP), an oral potassium channel blocker, has been used for several years as a treatment for numerous neurological diseases (Leussink *et al.*, 2018). Fampridine, an oral prolonged release 4-AP formulation is approved by the US Food and Drug Administration and European Medicines Agency for the symptomatic treatment of walking disability (Expanded Disability Status Scale, EDSS 4–7) in multiple sclerosis, and reportedly improves motor skills, walking ability and walking speed (Goodman *et al.*, 2007, 2009, 2010, 2015; Hupperts *et al.*, 2016). Furthermore, 4-AP has been shown to improve visual function (Horton *et al.*, 2013) and fatigue (Morrow *et al.*, 2017), as well as cognition and depression (Broicher *et al.*, 2018). The principally accepted mode of action for 4-AP in multiple sclerosis is via the blockade of axonal voltage gated potassium (K_v) channels, thus enhancing axonal conduction (Bostock *et al.*, 1981). The blockage of K_v channels is of recent scientific interest; experimental K_v channel blockade reportedly inhibits T-cell activation (Schmalhofer *et al.*, 2002), as well as axonal demyelination and degeneration, in the context of experimental autoimmune encephalomyelitis (EAE) (Jukkola *et al.*, 2017). Therefore, we aimed to investigate the neuroprotective effects of 4-AP by using highly sensitive *in vivo* techniques, including optical coherence tomography (OCT) and visual function testing, in experimental models of optic neuritis and traumatic nerve injury as well as people with multiple sclerosis.

Material and methods

Cell culture and organotypic slice culture

Isolation and cultivation of retinal ganglion cells

Retinal cultures were prepared as previously described (Grozdanov *et al.*, 2010). A detailed protocol is provided in the Supplementary material. Retinal ganglion cell (RGC) cultures were treated with the indicated concentrations of 4-AP or ciliary neurotrophic factor (CNTF) as a positive control and incubated for 7 days, a time point at which apoptosis already occurred. As a reference for the initially seeded RGC numbers, some cultures were fixed 2 h after dissociation. RGCs were fixed for 30 min in 4% paraformaldehyde (PFA) and stained for βIII-tubulin. RGC numbers per well were then quantified and counted using a fluorescence microscope ($\times$200 magnification, Axio Observer D1, Zeiss). The values represent the mean ± standard error of the mean (SEM) of six wells per treatment group and two independent experiments.

Brain slice culture demyelination model

Organotypic slice cultures from the cerebellum were obtained as described previously (Lepka *et al.*, 2017). Briefly, the cerebellum of 10-day-old C57BL/6J mice was dissected and cut into 350 mm sagittal sections using a McIlwain tissue chopper (Gala Instruments). Slices were dissociated, washed for 15 min and plated on culture inserts

(Millipore Millicel®-CM). After culturing slices for 7 days *in vitro* (5% CO_2, 33°C), a 24 h incubation with 0.01, 0.1 and 1 mM 4-AP or 1 µM fingolimod was carried out, followed by toxic demyelination with 750 mM *S*-nitrosoglutathione (GSNO) for another 24 h. Morphological analysis was performed by fluorescence microscopy (BX51, Olympus).

Preparation of mouse oligodendrocytes

Mouse oligodendrocyte precursor cells (mOPCs) were isolated from the cortex and cerebellum of postnatal Day 2 mice (C57BL/6J mice of either sex). The isolation of cells was performed using Neural Tissue Dissociation Kit P (Miltenyi Biotec) according to the manufacturer's instructions. Cells were then sorted by magnetic-associated cell sorting using anti-A2B5 MicroBeads (Miltenyi Biotec). Cultivation was performed in Dulbecco's modified Eagle medium (DMEM)/F-12 medium supplemented with 8 mM HEPES, GlutaMAX™, 100 U/ml penicillin, 100 µg/ml streptomycin, B27 (GIBCO Life Technologies), FGF 1:1000 and PDGFα 1:1000 using dishes coated with 0.1 mg/ml poly-L-lysine (PLL).

Preparation of rat oligodendrocytes

The generation of primary rat OPCs (rOPCs) from postnatal Day 0 (P0) cerebral rat cortices (Wistar rats of either sex) was performed as previously described (Gottle *et al.*, 2010). OPCs were maintained in proliferation-supporting high-glucose DMEM-based Sato medium (Thermo Fisher Scientific) supplemented with 10 ng/ml recombinant human bFGF (PeproTech) and 10 ng/ml recombinant human PDGF-AA (R&D Systems). Alternatively, differentiation was initiated by Sato medium depleted of growth factors and supplemented with 0.5% foetal calf serum (PAA Laboratories).

Immunofluorescence and live cell imaging of oligodendrocyte precursor cells

Mouse OPCs were seeded in PLL-coated 96-well plates and incubated for 48 h with or without 4-AP (0, 1, 2.5, or 5 mM 4-AP) to analyse the translocation of nuclear factor of activated T cells (NFAT). Tumour necrosis factor α (TNF-α) (10 ng/ml) was used as a positive control. Cells were washed, fixed with 4% PFA, permeabilized (0.3% Triton™ X-100) and blocked (Roti®-Immunoblock, Carl Roth). Staining was performed with NFAT1 antibody (1:125, Millipore) and Cy3 anti-mouse antibody (1:500, Invitrogen). For the estimation of mOPC viability, cells were incubated with 0.1 and 1 mM 4-AP 24 h prior to glutamate treatment. Viability was quantitated 4 h after glutamate addition by caspase3 antibody staining (1:400, Cell Signaling), with Cy3 anti-rabbit (1:500, Invitrogen) used as a secondary antibody. Analysis was performed semi-automatically using a BD Pathway 855 device (Becton Dickinson).

For the viability assay of rOPCs, cells were seeded in 6-well plates and treated with 1 mM 4-AP or 5 mM tetraethylammonium (TEA) in differentiation medium 24 h before glutamate addition and fixed after 8 h. Staining was performed with anti-cleaved caspase-3 antibody (1:500, Cell Signaling). Differentiation analysis was performed by incubating rOPCs for 2 or 8 days in differentiation medium with 1 mM 4-AP before fixation and staining with anti-MBP (myelin basic protein) antibody (1:500, Millipore). Analysis of immunofluorescence was performed by fluorescence microscopy (Carl Zeiss, ZEISS ZEN Digital Imaging).

Calcium live cell imaging was performed by seeding mOPCs in 96-well imaging plates coated with PLL 24 h before measurement at 100 000 cells/well. Fura2-AM (5 µM, Molecular Probes) in Hanks' balance salt solution was added 30 min before treatment with 0.1 and 1 mM 4-AP or vehicle. Measurements were performed with a BD Pathway 855 high-content imaging microscope (Becton Dickinson) with excitation at 340 nm and 380 nm for ratiometric analysis. Images were captured every 5 s for 200 s to calculate the Fura2 ratio.

Animal experiments and histological analysis

Experimental autoimmune encephalomyelitis-optic neuritis and treatment with 4-AP and fingolimod

EAE was induced by subcutaneous injection of 200 µg myelin oligodendrocyte glycoprotein fragment 35-55 (MOG_{35-55}, Biotrend) and 200 ng pertussis toxin (Sigma-Aldrich) twice (at Days 0 and 2) as previously described (Dietrich *et al.*, 2018). 4-AP stock solution was prepared at 0.5 M in phosphate-buffered saline (PBS; GIBCO Life Technologies), fingolimod stock solution at 100 µM in dimethyl sulfoxide (DMSO, Sigma-Aldrich) and stored at −80°C until use. Treatment started 1 week before the induction of EAE by adding 4-AP, fingolimod or both stock solutions for verum therapy or PBS/DMSO alone for vehicle control to the drinking water. Drinking water was replaced twice a week, uptake was measured daily, and the concentrations of the substances were adjusted to a daily treatment dose of 12.5 mg/kg body weight 4-AP or 3 mg/kg body weight fingolimod per day. The clinical EAE score was graded daily as previously described (Dietrich *et al.*, 2018). In brief, the following score was used: (0) no disease, (0.5) mild tail paresis, (1) obvious tail paresis or plegia, (1.5) tail plegia and no righting reflex, (2) mild signs of hind limb paresis with clumsy gait, (2.5) obvious signs of hind limb paresis, (3) hind limb plegia (dragging one hind limb behind), (3.5) hind limb plegia (dragging both hind limbs behind), (4) mild signs of quadriparesis, (4.5) quadriplegia, and (5) death or moribund.

T cell proliferation assay

EAE was induced and mice were treated with 4-AP or vehicle as described above. Splenocytes were isolated 14 days after EAE induction and cultured in RPMI medium, supplemented with 5% foetal bovine serum, 1% glutamine, 0,1% β-mercaptoethanol. T cells were stimulated by MOG_{35-55} (100, 50, 10, 2 and 0 µg/ml) or CD3 (1 µg/ml) as positive

control and incubated for 72 h. In the last 24 h of incubation, proliferation was assessed by bromodeoxyuridine staining and spectrophotometric analysis using by the BrdU Cell Proliferation ELISA Kit (colorimetric) (Abcam) according to the manufacturer's protocol.

Optic nerve crush

Mice were anaesthetized by intraperitoneal injections of ketamine (120 mg/kg) and xylazine (16 mg/kg). The left optic nerve was intraorbitally crushed 1 mm behind the eyeball for 10 s using jeweller's forceps (Hermle) as previously described (Leibinger *et al.*, 2009). The contralateral optic nerve served as a control. 4-AP and fingolimod treatment was performed as described above starting 7 days before the crush.

Optical coherence tomography in mice

OCT measurements were performed with a Spectralis[TM] HRA + OCT device (Heidelberg Engineering) under ambient light conditions as previously described (Dietrich *et al.*, 2017, 2018, 2019) and in detail in the Supplementary material.

Optokinetic response for visual function analysis

Optokinetic response (OKR) analysis was carried out in mice using a testing chamber and OptoMotry[TM] software (CerebralMechanics[TM]) (Prusky *et al.*, 2004) assessing the spatial frequency at 100% contrast as previously described (Dietrich *et al.*, 2018).

Tissue sampling and histological analysis

Perfusion, tissue sampling and analysis were performed as previously described (Dietrich *et al.*, 2018) and are reported in detail in the Supplementary material. At least four sections of the optic nerve, exclusively of the right eye of each mouse, were analysed per staining. The entire longitudinal section of each optic nerve was included for rating and intensity measurements.

Electron microscopy

For transmission electron microscopy (TEM), mice were sacrificed and transcardially perfused with 2% PFA and 2.5% glutaraldehyde 120 days after immunization. Optic nerves were dissected and incubated in 2% PFA and 2.5% glutaraldehyde at 4°C for 3 h and 1% osmium tetroxide for 2 h. Acetone at increasing concentrations was used for dehydration. After the block contrast was applied (1% phosphotungstic acid/0.5% uranyl acetate in 70% acetone), a SPURR embedding kit (Serva) was used according to the manufacturer's protocol. An Ultracut EM UC7 (Leica) was used to obtain ultrathin sections of 70 nm, followed by staining with lead citrate solution and 1.5% uranyl acetate. Images were captured at various magnifications using a TEM H7100/100KV (Hitachi) using a Moroda SIS Camera system and were subsequently processed by Olympus ITEM 5.0 Software.

Patients

Study population

The effects of an ongoing treatment with 4-AP on retinal degeneration in multiple sclerosis patients were analysed retrospectively by comparing longitudinal OCT datasets from patients with multiple sclerosis taking 4-AP for amelioration of walking disability to those from matched multiple sclerosis patients without 4-AP treatment. The inclusion criteria were: (i) diagnosis of multiple sclerosis according to the 2010 McDonald criteria (Polman *et al.*, 2011); (ii) availability of at least two longitudinal OCT datasets >6 months apart; and (iii) continuous 4-AP therapy between OCT scans or a matched control for a 4-AP patient according to the matching algorithm (see below). The exclusion criteria were confounding ocular pathologies or insufficient scan quality according to the OSCAR-IB criteria (Tewarie *et al.*, 2012). All demographic data were collected and analysed (Table 1). Controls were identified from the databases of the participating centres using a predefined hierarchical matching algorithm of seven items to stratify for possible confounders as follows: (i) multiple sclerosis subtype (relapsing remitting, primary progressive, secondary progressive); (ii) treatment with disease-modifying medication (DMT) categories [none, active (natalizumab, rituximab, alemtuzumab, fingolimod), baseline (glatiramer acetate, dimethyl fumarate, teriflunomide, interferon beta), mitoxantrone/cyclophosphamide]; (iii) disease duration category at baseline OCT (<5 years, 5–10 years, >10 years); (iv) peripapillary retinal nerve fibre layer (RNFL) percentile (≤77 μm, 77–92 μm, >92 μm); (v) age category at baseline OCT (18–29 years, 30–39 years, 40–49 years, ≥50 years); (vi) exact DMT; and (vii) sex. Items i–iii were mandatory criteria for matching; iv–vii were optional criteria to decide between several possible matches.

Optical coherence tomography in human patients

The OCT methodology reported is in line with the APOSTEL recommendations (Cruz-Herranz *et al.*, 2016). All except one centre used a Spectralis[TM] OCT (Heidelberg Engineering) device to obtain OCT scans under ambient light conditions as previously described (Albrecht *et al.*, 2012). Data from Johns Hopkins University were obtained by a spectral-domain Cirrus HD-OCT (model 4000, software version 6·0; Carl Zeiss Meditec) as described elsewhere (Warner *et al.*, 2011). To assess the peripapillary RNFL, we performed circular ring scans with a diameter of 3.4 mm (100 A-scans). The centre of the circle was positioned manually in the middle of the optic disc. High-resolution, horizontal volume scans were centred in the middle of the fovea. The high-resolution mode was used; all scans had a quality of at least 20 dB (see Supplementary Table 1 for detailed information on OCT used at the centres).

Analysis was performed as described above in mice using automated segmentation by Heidelberg Eye Explorer[TM] software and an open source segmentation algorithm (Bhargava *et al.*, 2015) for Spectralis and Cirrus scans, respectively, followed by manual correction by a blinded investigator.

Table 1 Demographic and clinical data at baseline visit

	4-AP	Control	Statistics
n	52	51	
Age[a], years, mean ± SEM	53.23 ± 0.875	50.71 ± 0.852	$t(204) = -2.066$; $P = 0.040$; two-tailed
Sex[c], % female	65.4	68.6	$\chi^2(1) = 0.245$; $P = 0.621$
Multiple sclerosis type			
% RRMS	15.4	15.7	$\chi^2(2) = 0.571$; $P = 0.752$
% PPMS	38.5	43.1	
% SPMS	46.2	41.2	
Disease duration, years, mean ± SEM	13.58 ± 0.903	13.45 ± 0.859	$t(204) = -0.102$; $P = 0.919$; two-tailed
EDSS[b]			
Mean	4.895	4.610	$U = 2824$; $z = -1.025$; $P = 0.305$
Median	5	4	
n	38	41	
p-RNFLT tertile			
% 1 ($<77\ \mu m$)	30.7	35.	$\chi^2(2) = 0.611$; $P = 0.737$
% 2 (77–$92\ \mu m$)	33.7	33.3	
% 3 ($>92\ \mu m$)	35.6	31.3	
Baseline medication category[d]			
% None	51.9	60.8	$\chi^2(3) = 3.317$; $P = 0.345$
% Active	21.2	19.6	
% Baseline	17.3	15.7	
% Mito/cyclo	9.6	3.9	

[a]Age and disease duration were compared using two-tailed t-test.
[b]The Expanded Disability Status Scale (EDSS) was compared with the Mann-Whitney U-test.
[c]All other parameters were compared using chi-square testing.
[d]Concomitant disease-modifying therapy category: none, active (natalizumab, rituximab, alemtuzumab, fingolimod), baseline (glatiramer acetate, dimethyl fumarate, teriflunomide, interferon beta), mitoxantrone/cyclophosphamide (Mito/cyclo).
PPMS = primary progressive multiple sclerosis; pRNFLT = peripapillary RNFL thickness; RRMS = relapsing remitting multiple sclerosis; SPMS = secondary progressive multiple sclerosis.

The mean thicknesses were calculated for the peripapillary RNFL (circular ring scans), as well as the macular RNFL, ganglion cell inner plexiform layer (GCIPL) (complex of GCL + IPL) and total retinal thickness were obtained from volume scans using the 1, 3 and 6 early treatment of diabetic retinopathy study grid excluding the central 1 mm diameter area (fovea).

Statistical analysis

All statistical analyses were performed using SPSS Statistics 20.0.0 (IBM) or Prism 5.0 (GraphPad) and are described in detail in the Supplementary material.

Study approval

Patients

The retrospective clinical study and data contribution was approved by all local ethics committees and the main study by the Heinrich-Heine University Düsseldorf (study number 4228R, registration ID 2015114593). Written informed consent was obtained from all patients.

Patients from Düsseldorf, Zürich, San Francisco, Baltimore, Barcelona, and Munich and Berlin were included in this retrospective longitudinal study.

Animals

All animal experiments were carried out in female 6-week-old C57BL/6J mice (Janvier Labs). The procedures were performed in compliance with the 'Animal Research: Reporting of In Vivo Experiments' (ARRIVE) guidelines, approved by the regional authorities (State Agency for Nature, Environment and Consumer Protection; AZ 84-02.4.2014.A059) and conformed to the Association for Research in Vision and Ophthalmology (ARVO) Statement for the Use of Animals in Ophthalmic and Vision Research.

Data availability

All data are available upon request by a qualified researcher.

Results

Clinical score and visual function in experimental autoimmune encephalomyelitis-optic neuritis

In the first set of experiments, prophylactic 4-AP treatment of EAE-optic neuritis (EAEON) in mice was performed using immunomodulatory treatment with fingolimod as a positive control (Choi et al., 2011; Rossi et al., 2012). The clinical score was attenuated when mice were treated with either

4-AP or fingolimod (Fig. 1A). Similarly, the degeneration of the inner retinal layer, assessed *in vivo* by OCT, was reduced under treatment with 4-AP or fingolimod (Fig. 1B). These results were in line with the reduced loss of RGCs determined by post-mortem staining of retinal whole mounts

(Fig. 1C–E). Interestingly, OCT and histology revealed continuous degeneration of inner retinal layer and RGCs, respectively, which was still ongoing until at least 120 days (Fig. 1C–E). Visual function, measured by the optokinetic response, provided further support on a functional level for
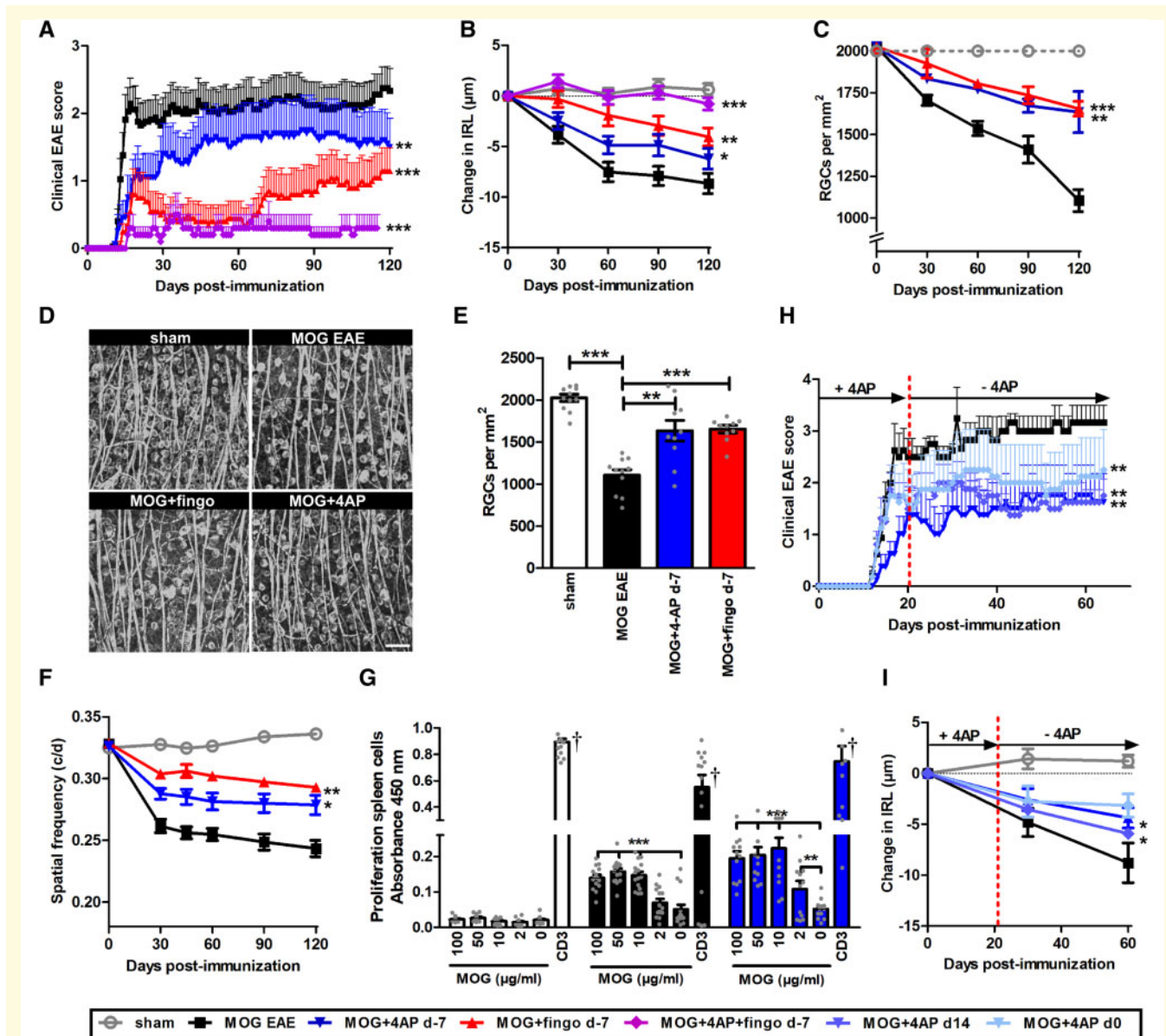

Figure 1 4-AP attenuates MOG$_{35-55}$-induced EAE in C57BL/6J mice also after withdrawal. (A) Clinical EAE score and **(B)** degeneration of the inner retinal layers of female C57BL/6J EAE mice. **(C)** Number of RGCs over 120 days of EAE. **(D)** At 120 days after EAE induction, eyes were enucleated, retinae were isolated, and RGCs were stained with βIII-tubulin antibody. Scale bar = 50 μm. **(E)** The bar graph shows the RGC density 120 days after immunization. **(F)** The spatial frequency (c/d) reflecting the visual function of EAE mice over 120 days. **(G)** Spleen cells from EAE mice, isolated 14 days after immunization, were restimulated with increasing concentrations of MOG$_{35-55}$, CD3 as positive control. **(H)** EAE scores and **(I)** inner retinal layer (IRL) thickness change with 4-AP withdrawal after 21 days. Substances were administered either 7 days before (d-7), on the same day (d0) or 14 days after (d14) immunization, 4-AP at 250 μg/mouse/day or fingolimod (fingo) at 3 mg/kg body weight per day. All graphs represent the pooled mean ± SEM; grey dots indicate individual datapoints (**A–F**, *n* = 12 animals per group out of three independent experiments; **H** and **I**, *n* = 8 animals per group out of two independent experiments) with *$P < 0.05$; **$P < 0.01$; ***$P < 0.001$, area under the curve compared by GEE or ANOVA with Dunnett's *post hoc* test for time courses compared to untreated MOG EAE. **$P < 0.01$; ***$P < 0.001$, by ANOVA with Dunnett's *post hoc* test compared to MOG EAE untreated mice for the bar graph. †Few datapoints out of axis limits.

the observed structural atrophy with a similar curve of progression. Spatial frequency was reduced to 0.24 cycles per degree (c/d) after 120 days of EAEON, while mice under 4-AP or fingolimod treatment retained a spatial frequency of 0.28 and 0.29 c/d, respectively (Fig. 1F). Hence, functional and structural *in vivo* readouts were in accordance and corresponded to the histological findings. To exclude an effect of 4-AP on the induction of T-cell-mediated immunization, splenocytes from EAE mice were isolated 14 days after immunization and restimulated with MOG_{35-55} at increasing concentrations. No significant differences were observed between vehicle-treated EAE mice and animals pretreated (7 days before immunization) with 4-AP (Fig. 1G).

As fingolimod and 4-AP likely have different modes of action, we also investigated the effect of combination therapy with both drugs in the EAEON. With combination therapy, an additive beneficial effect was observed, resulting in diminished mean disability below a clinical score of 0.5 (Fig. 1A). Inner retinal layer degeneration was almost completely prevented during 120 days of the EAE disease course when both substances were administered together (Fig. 1B).

As 4-AP is primarily considered a symptomatic treatment improving axonal signal transduction by blocking potassium channels, we also treated animals with 4-AP and discontinued the treatment 21 days after MOG_{35-55} immunization. Indeed, the clinical disease score indicated a slight decline after withdrawal, confirming a symptomatic treatment effect component. However, even after 60 days, EAE scores remained attenuated in 4-AP-treated mice compared to vehicle-treated EAE control mice (Fig. 1H). To assess the appropriate timing of treatment administration, we compared the efficacy of 4-AP treatment provided at different time points during EAE. The clinical EAE scores were still attenuated relative to vehicle treatment when a late prophylactic 4-AP treatment starting at EAE induction (Day 0) or a therapeutic treatment at the first peak of disease (Day 14) were performed, albeit less pronounced than those for early prophylactic treatment with 4-AP (Day –7) (Fig. 1H). Interestingly, at 30 and 60 days, inner retinal layer thinning showed no significant difference between the different treatment starting point paradigms (Fig. 1I).

Optic nerve crush

Optic nerve crush is considered a model of traumatic axonal injury, thus primarily involving non-inflammatory axonal damage. As EAEON is a rather inflammatory-driven model, we used it to gather information about the possible protective modes of action of 4-AP and fingolimod occurring independently of immunomodulatory effects (Fig. 2A). Three weeks after the optic nerve was crushed in 6-week-old C57BL/6J mice, the number of RGCs, stained by a βIII-tubulin antibody (Fig. 2B), was higher in animals under 4-AP treatment (449 ± 23.8 cells/mm²) compared to vehicle-treated controls (362 ± 22.5 cells/mm²), while prophylactic fingolimod treatment did not result in enhanced cell survival (375 ± 17.5 cells/mm²) (Fig. 2C).

Ganglion cell cultures

To investigate whether the effects of 4-AP treatment resulted from direct neuroprotective properties, we isolated RGCs from mouse retinas and cultured the cells for 7 days. Compared with vehicle treatment, 4-AP treatment did not lead to improved survival of these axotomized neurons, while a concentration of 1 mM 4-AP even had toxic potential (Fig. 2D). RGCs isolated from mice pretreated with 12.5 mg/kg per day 4-AP *in vivo* for 7 days also showed no enhanced survival under continued 4-AP therapy *in vitro* for another 7 days (Fig. 2E). The functionality of the assays was verified by treatment with 10 nM CNTF, which significantly increased RGC survival (Mey and Thanos, 1993).

Optic nerve histology of experimental autoimmune encephalomyelitis mice

After 120 days of MOG_{35-55}-induced EAE, optic nerves were immunolabelled for CD3, Iba1 and MBP (Fig. 3A) to analyse the effects on T-cell infiltration, microglial activation and myelin status, respectively. The optic nerves from untreated EAE mice showed large areas of demyelination, while demyelination in EAE mice treated with fingolimod and 4-AP was significantly reduced. Moreover, immunomodulatory therapy with fingolimod caused a reduction in microglial activation and the number of T cells in optic nerves, while 4-AP did not lead to any of these anti-inflammatory effects (Fig. 3B).

To confirm the effects of 4-AP on the myelin sheath, observed by MBP staining, we performed TEM of ultrathin cross sections to evaluate the ultrastructure of the optic nerve from sham and EAE mice. Macroscopic analyses revealed that the prominent decrease of myelinated axons and destruction of the myelin structure, occurring in EAE mice 120 days after immunization, was diminished in optic nerves of mice pretreated (Day –7) with 4-AP. Sham-immunized animals showed a normal myelin configuration (Fig. 3C). A quantitative analysis of the myelin thickness revealed a significantly higher myelin-axon ratio in 4-AP treated, compared to vehicle-treated EAE mice (Fig. 3D).

Brain slice cultures

The potential of 4-AP to protect against demyelination was confirmed *in vitro* in brain slice cultures isolated from C57BL/6J mice. Demyelination was induced by exposure to the physiological nitric oxide donor GSNO to mimic activation of microglia, while the slices were treated either with vehicle, 4-AP or fingolimod (Fig. 3E). The degree of structural white matter and myelin damage was significantly less severe in 4-AP-treated slices than in control slices, while fingolimod did not show any protective effects against GSNO-mediated demyelination. Interestingly, *in vitro*, concentrations of 1 mM were required to protect myelin structure, while lower concentrations were ineffective (Fig. 3F)
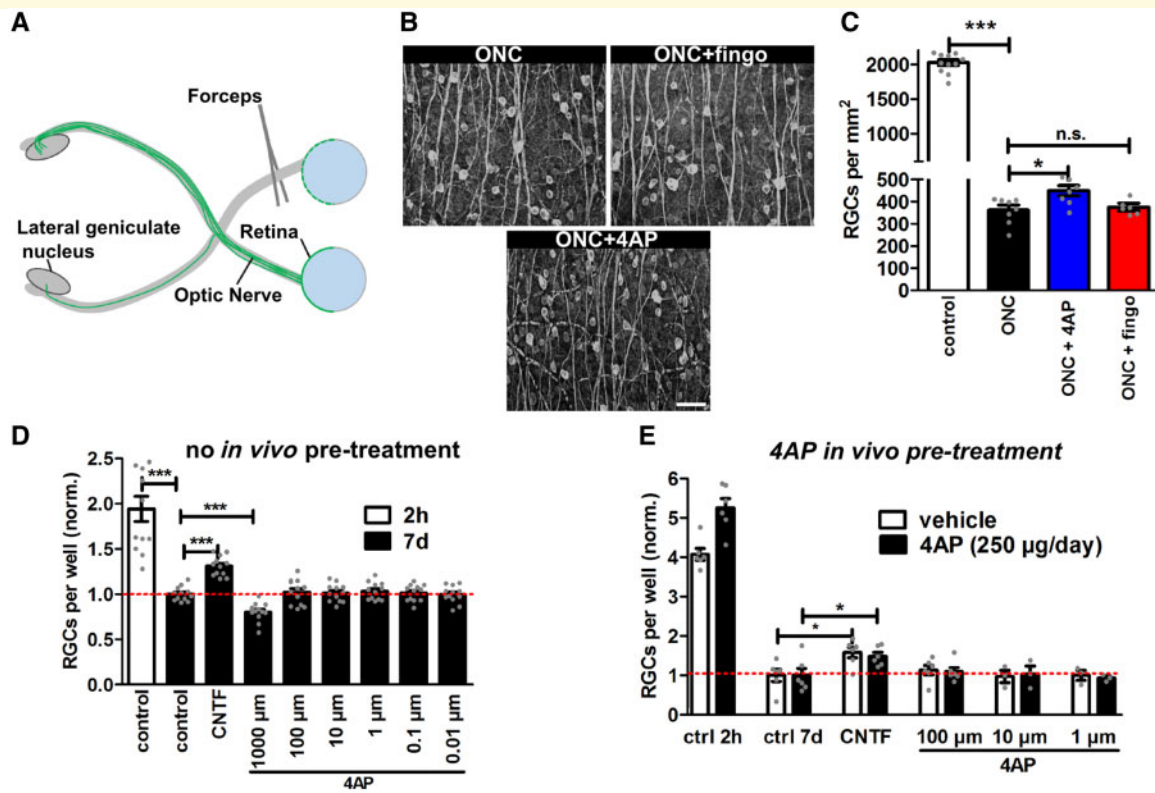
Figure 2 4-AP does not directly affect the neuroprotection of axotomized RGCs. (**A**) Schematic image of optic nerve crush. (**B**) Cells were stained with βIII-tubulin antibody 3 weeks after optic nerve crush. Scale bar = 50 µm. (**C**) RGC density of C57BL/6J mice 3 weeks after optic nerve crush. Mice were treated with 4-AP at 250 µg/mouse/day, fingolimod at 3 mg/kg body weight/day or vehicle control. (**D**) Survival of isolated RGCs *in vitro* under 4-AP treatment. (**E**) RGC survival isolated from C57BL/6J mice pretreated with 4-AP for 7 days (250 µg/mouse/day); CNTF as a positive control. All graphs represent the pooled mean ± standard deviation (SD). Grey dots show individual data-points (**B** and **C**, n = 6 animals per group out of two independent experiments; **D** and **E**, eyes from n = 3 mice per group) with *$P < 0.05$; ***$P < 0.001$, n.s. = not significant, by ANOVA with Dunnett's *post hoc* test compared to untreated controls. [†]One datapoint out of axis limits.

Oligodendroglial cell cultures

The effects of 4-AP in EAE, optic nerve crush and *in vitro* experiments indicated the involvement of oligodendroglial cells. Therefore, the protective potential of 4-AP on mOPCs was analysed using a viability assay. Vehicle-treated mOPCs displayed rather high caspase activity even under standard culture conditions, which increased under glutamate-induced stress. However, compared to vehicle treatment, 4-AP treatment of mOPCs led to significantly reduced caspase activity both with and without glutamate stress (Fig. 4A).

To investigate the mode of action further, we analysed the nuclear translocation of several transcription factors involved in cell survival after 48 h of 4-AP treatment in mOPCs. We observed no changes for nuclear factor erythroid 2-related factor 2 (Nrf2) (Supplementary Fig. 1).

In contrast, we observed an increased nuclear translocation of NFAT in these cells at concentrations from 1 mM 4-AP, while increasing concentrations of 4-AP were less effective (Fig. 4B). As NFAT is dependent on cellular calcium homeostasis, we used Fura2-based calcium imaging to investigate this relationship further. 4-AP treatment of mOPCs resulted in a rapid calcium influx into the cytosol (Fig. 4C).

To exclude species effects, we also investigated the effects of rOPCs isolated from Wistar rats. The beneficial effects of 4-AP on the survival of these cells were also detected. Interestingly, rOPCs demonstrated a lower baseline activation of caspase-3 in their standard cell culture medium, which was unaffected by 4-AP. However, similar to mOPCs, treatment with 1 mM 4-AP significantly reduced the activation of caspase-3 under glutamate stress in rOPCs (Fig. 4D and E).

To investigate whether 4-AP treatment affects the differentiation of OPCs, we performed MBP staining at 2 and 8 days after preparation of rOPCs to assess early and late differentiation, respectively (Fig. 4F). The differentiation at both time points was not altered under 4-AP treatment (Fig. 4G). To analyse the role of potassium channels as the presumed primary target of 4-AP, we used the K_v channel blocker TEA, which has targets similar to those of 4-AP, with both substances blocking a wide range of K_v channel subtypes. However, incubation with 1 mM TEA did not lead to any protective effects in rOPCs as
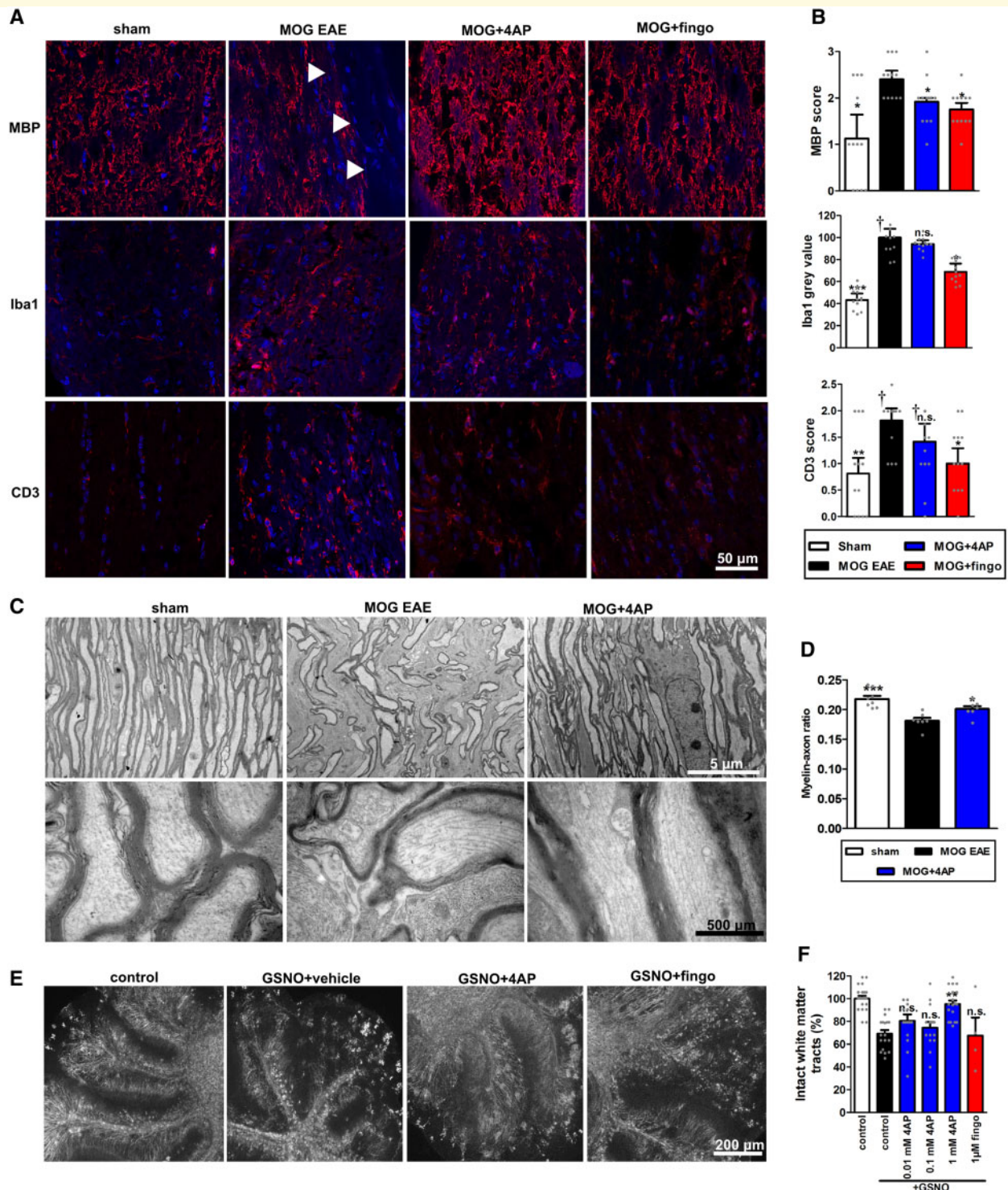
Figure 3 Effects of 4-AP are non-inflammatory driven and prevent demyelination. (**A**) Longitudinal sections of optic nerves of mice with sham, MOG EAE and MOG EAE with 3 mg/kg body weight fingolimod or 250 µg/mouse/day 4-AP treatment stained for MBP, Iba1 and CD3; arrows indicate areas of demyelination. (**B**) Quantitative analyses of myelin status (MBP score), microglial activation by fluorescence intensity measurement and T-cell infiltration (CD3 score). One optic nerve per mouse was included. (**C**) Representative TEM images of longitudinal optic nerve sections from sham, MOG EAE and MOG EAE with 250 µg/mouse/day 4-AP treated C57Bl/6J mice. (**D**) Quantitative determination of the myelin-axon ratio, calculated by the thickness of the myelin sheath and the axon. (**E**) Representative images of brain slice cultures of GFP-myelin mice with and without GSNO treatment. (**F**) Quantitative results of myelin damage. All graphs represent the pooled mean ± SEM; grey dots show individual datapoints (**A** and **B**, n = 12 animals per group out of three independent experiments; **C** and **D**, slices from n = 13 animals per group; **E** and **F**, slices from n = 5 animals per group) with *$P < 0.05$, **$P < 0.01$, ***$P < 0.001$, n.s. = not significant, by ANOVA with Dunnett's *post hoc* test compared to MOG untreated mice for optic nerves and compared to GSNO treated slices for brain slice cultures. [†]Few datapoints out of axis limits.
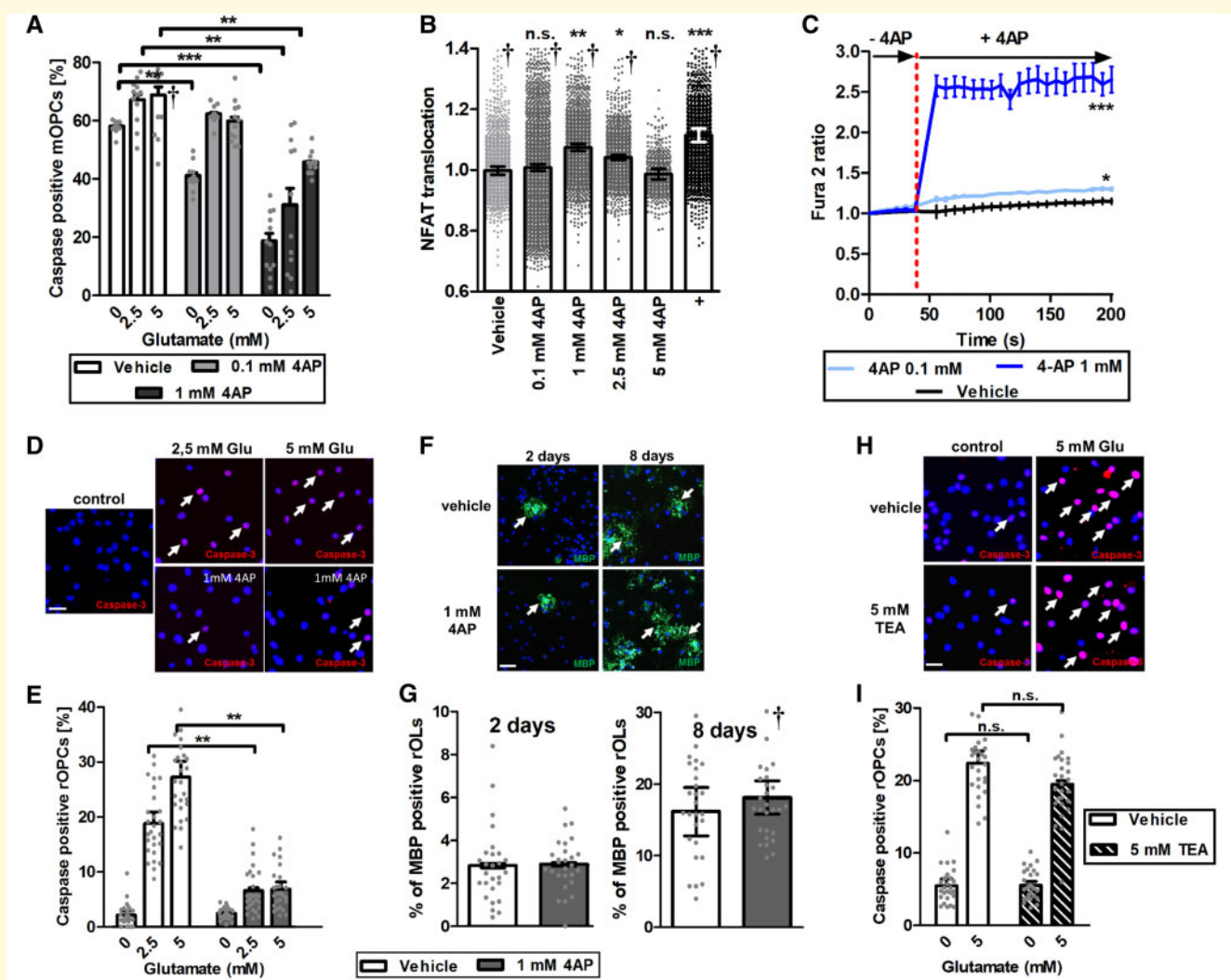
Figure 4 Effects of 4-AP are based on NFATc1 translocation in OPCs but do not affect differentiation and might be independent of K$_v$ channel blocking. (A) Quantitative analysis of caspase-stained mouse OPCs in a glutamate toxicity assay. **(B)** Nuclear translocation of the NFATc1 transcription factor under 4-AP treatment in mOPCs, plus symbol = 10 ng/ml TNF-alpha. **(C)** Calcium influx of mOPCs after incubation with 4-AP measured by Fura2 dye. **(D)** Caspase staining of rat OPCs in a glutamate toxicity assay with 1 mM 4-AP. **(E)** Percentage of caspase-positive cells in a glutamate assay at 1 mM 4-AP in the medium. **(F)** MBP-stained rat oligodendrocytes in differentiation medium 2 and 8 days after cell preparation. **(G)** Analysis of MBP synthesis in 2- and 8-day-old rat oligodendrocytes (rOLs). **(H)** Caspase staining of rOPCs after TEA treatment in a glutamate assay. **(I)** Caspase-positive rOPCs after TEA treatment, glutamate was added to induce oxidative stress. Scale bars = 30 μm. All graphs represent the pooled mean ± SEM. Grey dots show individual datapoints ($n = 12$ out of three separate experiments), with *$P < 0.05$, **$P < 0.01$, ***$P < 0.001$, n.s. = not significant, by ANOVA with Dunnett's *post hoc* test compared to vehicle-treated control or as indicated for bar graphs; * $P < 0.05$, ***$P < 0.001$, area under the curve compared by ANOVA with Dunnett's *post hoc* test for time courses. †Some datapoints out of axis limits.

observed with 4-AP treatment, suggesting that the effect is unlikely to be mediated by potassium channel blocking alone (Fig. 4I).

Longitudinal retinal neurodegeneration in patients with multiple sclerosis

As sustained-release 4-AP is licensed and used for the symptomatic treatment of multiple sclerosis, we aimed to

investigate whether 4-AP exerts retinal neuroprotective effects in patients with multiple sclerosis similar to those observed in our abovementioned preclinical models. In a retrospective, longitudinal, international multicentre study, we identified 52 patients receiving continuous 4-AP therapy and concurrent longitudinal OCT monitoring, as well as 51 non-4-AP-treated matched controls (see Supplementary Fig. 2 for detailed illustration of the inclusion process and number of included eyes). The baseline and second visit were 14.8±0.6 months apart for 4-AP patients, and 16.6±0.9

months for control patients ($P = 0.105$, two-tailed t-test). The time interval between the baseline and second visit averaged 28.2 ± 1.3 months for 4-AP patients and 32.0 ± 2.0 months for control patients ($P = 0.126$, two-tailed t-test). 4-AP and control patients differed significantly in age (Table 1); however, we adjusted for age in the generalized estimation equation (GEE) analysis.

In both groups, the mean peripapillary RNFL, total retinal and macular RNFL and GCIPL thicknesses decreased over the course of 12 and 24 months (Table 2 and Fig. 5). The mean total retinal thickness did not differ between the groups ($P = 0.512$ and $P = 0.330$ after 12 and 24 months, respectively) and showed significant thinning over time in 4-AP-treated patients after 12 months ($P = 0.009$, GEE) as well as in the control group after 24 months ($P = 0.001$, GEE).

The thickness reduction in the macular RNFL (Fig. 5B) was greater in the control group over the course of 12 and 24 months than in the 4-AP-treated group at these time points ($P = 0.011$ and $P < 0.001$, respectively; Table 2). The macular GCIPL thickness reduction after 12 months was significantly different from the baseline thickness in 4-AP patients ($P = 0.024$, GEE) and after 24 months in the control group ($P = 0.009$, GEE); however, there was no significant difference between the groups (Table 2 and Fig. 5C).

Peripapillary RNFL thickness significantly decreased over time in the 4-AP treatment group (after 12 and 24 months from baseline, $P = 0.009$ and $P = 0.013$) and was also significantly different from baseline after 24 months in the control group ($P = 0.041$, GEE), with no significant difference in group comparisons.

In sub-analyses also controlling for history of optic neuritis >6 months before the baseline OCT and for clinical relapses other than ON during the observational period the results of the main analysis were not changed. History of optic neuritis only had a significant influence on the baseline thicknesses (each $P < 0.001$, GEE).

The median EDSS did not change over time (12 months versus baseline: $P = 0.096$ for 4-AP and $P = 0.380$ for controls; 24 months: $P = 0.120$ for 4-AP and 0.078 for controls, Wilcoxon test) and did not show any significant difference between study groups ($P = 0.814$ after 12 months and $P = 0.931$ after 24 months, Mann-Whitney U-test). However, a higher EDSS at 12 months was associated with a significantly thinner macular total retinal thickness and macular RNFL at 12 months in the control cohort (macular total retinal thickness: B = -0.441, $P = 0.002$; macular RNFL: B = -2.032, $P < 0.001$; GEE) but not in the 4-AP cohort (macular total retinal thickness: B = 2.443, $P = 0.310$; macular RNFL: B = 0.995, $P = 0.095$; GEE).

Discussion

Our finding of the indirect neuroprotective effects of 4-AP may have an immense impact on multiple sclerosis treatment strategies if confirmed in a prospective randomized
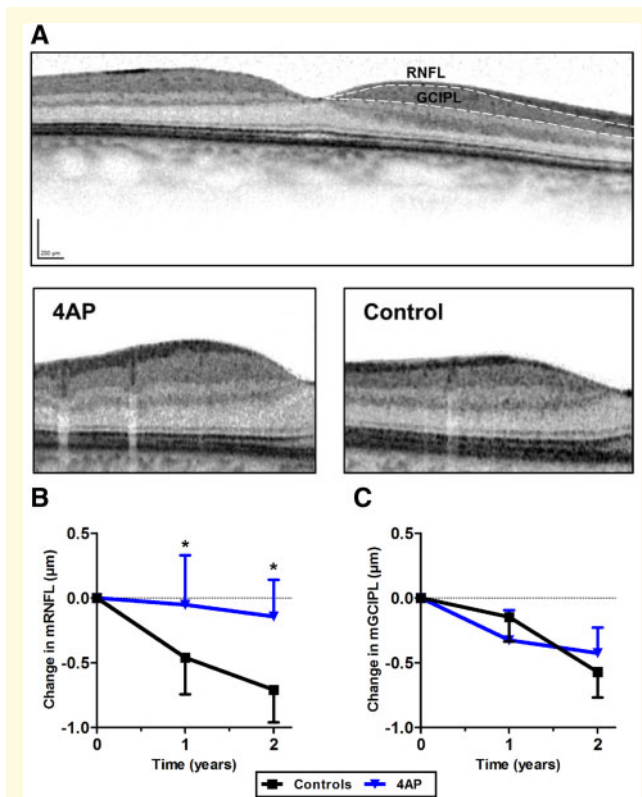

Figure 5 Effects of 4-AP on the retinal layers in multiple sclerosis patients. (**A**) The macular RNFL (mRNFL) and complex of the GCIP (mGCIPL) were automatically segmented in volume scans, and obvious errors were manually corrected. Thickness changes over the course of 2 years for (**B**) macular RNFL and (**C**) macular GCIPL are displayed. Graphs represent the means for both groups ± SEM, using GEE models with *$P < 0.05$.

controlled clinical trial. In multiple sclerosis, although the arsenal of immunomodulatory therapies is continuously increasing, effective treatment strategies for axonal and neuronal degeneration, the principal substrates of permanent disability (Reich *et al.*, 2018), are lacking. Our preclinical data demonstrate that prophylactic and early therapeutic 4-AP treatment reduce neuroaxonal and visual loss, as well as clinical disability, in EAEON, primarily by acting on myelin and oligodendrocytes. These effects seem to be independent of an interference of 4-AP during EAE induction, validated by a T-cell restimulation assay. Most importantly, we provide evidence that 4-AP can strongly augment the beneficial effects of prophylactic immunomodulatory treatment with fingolimod, resulting in almost no degeneration of inner retinal layers. It is reasonable to assume that this effect is not limited to fingolimod alone and applicable to 4-AP combined with other multiple sclerosis immunomodulatory therapies. Protective efficacy was demonstrated *in vivo* across several independent functional and structural readouts, including the clinical EAE score, visual function, *in vivo* retinal imaging and histological staining of RGCs, supporting the validity of these data. Furthermore, 4-AP

Table 2 OCT results for patients with multiple sclerosis

Time point	4-AP	Control	Statistics GEE 4-AP versus Control
Peripapillary RNFL, μm^a			
Baseline[b]	85.50 ± 1.412	83.72 ± 1.441	$P = 0.885; n = 100/99$
Δ12 months	-0.631 ± 0.319 ($P = \mathbf{0.004}$)	0.270 ± 0.639 ($P = 0.398$)	$P = 0.798; n = 98/97$
Δ24 months	-1.810 ± 0.417 ($P = \mathbf{0.013}$)	0.320 ± 1.208 ($P = \mathbf{0.041}$)	$P = 0.137; n = 42/51$
Mean TRT, μm^a			
Baseline	298.642 ± 2.369	292.943 ± 2.593	$P = 0.981; n = 62/60$
Δ12 months	-1.595 ± 0.618 ($P = \mathbf{0.009}$)	-0.976 ± 0.630 ($P = 0.102$)	$P = 0.512; n = 61/59$
Δ24 months	-1.351 ± 0.600 ($P = 0.188$)	-2.064 ± 0.451 ($P = \mathbf{0.001}$)	$P = 0.330; n = 28/29$
Macular RNFL, μm^a			
Baseline	30.325 ± 0.741	30.683 ± 0.764	$P = \mathbf{0.046}; n = 61/60$
Δ12 months	0.068 ± 0.198 ($P = 0.827$)	-0.253 ± 0.157 ($P = 0.050$)	$P = 0.011; n = 60/59$
Δ24 months	-0.022 ± 0.267 ($P = 0.939$)	-0.622 ± 0.220 ($P = 0.143$)	$P < \mathbf{0.001}; n = 27/29$
Macular GCIPL, μm^a			
Baseline	63.574 ± 0.885	63.735 ± 0.986	$P = 0.663; n = 97/99$
Δ12 months	-0.393 ± 0.164 ($P = \mathbf{0.024}$)	-0.236 ± 0.163 ($P = 0.409$)	$P = 0.213; n = 96/94$
Δ24 months	-0.230 ± 0.274 ($P = 0.760$)	-0.577 ± 0.191 ($P = \mathbf{0.009}$)	$P = 0.883; n = 45/50$

[a]Changes after 12 and 24 months compared to baseline were examined using GEE models, and the results are indicated in parentheses, significant differences compared to the control group are highlighted in bold ($P \leqslant 0.05$).
[b]The mean baseline values and annualized changes after 12 and 24 months are presented for each layer, the number of eyes for each measurement are indicated as n = 4-AP/matched control.
TRT = total retinal thickness.

prevented the degeneration of RGCs in the optic nerve crush model, while fingolimod was ineffective, providing additional evidence of the protective capacities of 4-AP.

Our study findings are in accordance with previous studies using 4-AP in models of peripheral nerve damage, which demonstrated increased recovery of nerve conduction velocity, promoted remyelination, and increased axonal area under prophylactic 4-AP treatment in sciatic nerve crush (Tseng *et al.*, 2016). However, previous literature on the effects of 4-AP in EAE is primarily heterogeneous. Oral and intraperitoneal 4-AP treatments with lower doses of 5 mg/kg and 250 µg/kg, respectively, reportedly increased walking ability assessed by the Rotarod and EAE scores of C57BL/6 mice; however, when administered from the day of immunization, the treatments did not influence the EAE score, cytokine profile or T-cell activation (Gobel *et al.*, 2013). In a more recent study, prophylactic oral treatment at higher doses of 30 mg/kg significantly improved EAE scores and reduced T-cell activation and Th1/17 polarization in proteolipid protein-induced EAE in SJL mice (Moriguchi *et al.*, 2018). Interestingly, this effect was not observed in MOG_{35-55} peptide-induced EAE in C57BL/6 mice; however, these mice were immunized with a far higher dose of MOG_{35-55} peptide than that used in our study (100 mg versus 200 µg) (Moriguchi *et al.*, 2018). These discrepancies may in part be explained by differences in dosing and treatment duration, as we performed the majority of our experiments with a prophylactic treatment starting 7 days before the induction of EAE. However, we also identified protection from retinal degeneration and less effective, but significant, mitigation of EAE scores when treatment began on the day of immunization and even at Day 14 after immunization. We

acknowledge that the doses in our EAE experiments are higher than the dose recommended for patients. We calculated the treatment dose following the 'Guidance for Industry Estimating the Maximum Safe Starting Dose in Initial Clinical Trials for Therapeutics in Adult Healthy Volunteers' published by the FDA in 2005, which suggests that the dose used in mice needs to be divided by 12.3 to convert it to the 'Human Equivalent Dose'. This taken into account, our dosing is only approximately three times higher than the dosing used in patients with multiple sclerosis.

Therefore, obtaining clinical data from patients to support these preclinical results is of great clinical interest, especially since 4-AP is already licensed and used in the symptomatic treatment of subsets of multiple sclerosis patients with walking disability (EDSS 4–7). Usually, 4-AP is discontinued if no direct symptomatic effect on walking tests such as the timed 25-foot walk test is observed. Therefore, it is beneficial to know whether 4-AP has additional disease-modifying effects, as it could then be offered to a wider range of patients. Clinical assessments of disability in routine practice are rather insensitive to change, therefore, an advantage of our preclinical investigations is that the approach of *in vivo* retinal imaging can be directly translated to clinical settings, given the increasing numbers of centres where OCT imaging is being performed in patients with multiple sclerosis on a routine basis. In a joint effort by the IMSVISUAL consortium (Balcer *et al.*, 2018), we were able to identify a group of 52 patients receiving continuous 4-AP therapy with longitudinal OCT datasets available and 51 matched non-4-AP-treated multiple sclerosis controls. A concern regarding retrospective analyses of this nature is indication bias, which can have a major impact on the composition of the

treatment groups. Although we used a predefined rigorous algorithm to match 4-AP-treated patients to non-4-AP-treated multiple sclerosis controls individually at all centres, yielding more homogeneous groups and reducing the risk of bias, it is important to recognize the need for a prospective assessment of the retinal neuroprotective effects of 4-AP, preferably in a randomized controlled fashion, to overcome the limitations of a retrospective approach. Moreover, the sample size was low for a study aiming to detect differences in atrophy rates for the inner retinal layers over 2 years in the absence of optic neuritis. Nonetheless, we were able to detect significantly lower rates of macular RNFL thinning in patients treated with 4-AP than in matched controls. Interestingly, the rates of peripapillary RNFL and GCIPL thinning did not differ significantly between the groups. The macular RNFL in volume scans, despite being thinner in the macular area, might be more sensitive to change than the peripapillary RNFL measured in ring scans around the disc (Albrecht *et al.*, 2017; Pietroboni *et al.*, 2017; Stellmann *et al.*, 2017). The macular RNFL reflecting axonal loss may unveil degeneration more rapidly than the GCIPL, which includes the neurons in the ganglion cell layer and their dendritic arbours in the IPL. Other possible explanations, such as axon-independent thickness loss in the macular RNFL (i.e. loss of oedema), or isolated protection of axons seem very unlikely given the preclinical findings. Regardless, it is clear that larger, prospective studies with longer follow-up times are warranted to more definitively corroborate the retinal neuroprotective effects of 4-AP in people with multiple sclerosis, as well as in the macular GCIPL and peripapillary RNFL. Notably, preclinical investigations were performed in a model of acute optic neuritis, while the clinical study focused on the slow chronic retinal degeneration occurring in the absence of optic neuritis. This was owing to the fact that 4-AP is licensed for the symptomatic treatment of walking disability, which occurs in the later phases of disease when optic neuritis is less likely to occur. However, a future randomized controlled trial, focusing on acute optic neuritis with higher rates of thinning over shorter times, would allow for the generation of meaningful results with smaller sample sizes and shorter follow-up times.

Our histological analysis of optic nerves after EAEON demonstrated that in contrast to fingolimod, 4-AP had no effect on the infiltration of T lymphocytes (CD3) or activated microglia and macrophages (Iba1). However, despite the lack of influence on inflammation, we still observed significant preservation of myelin (MBP) in the optic nerves of 4-AP-treated EAEON mice, reaching the same effect size as prophylactic fingolimod treatment. Additionally, we confirmed these findings by TEM, where we observed a more preserved myelin structure and a higher myelin-axon ratio in mice under 4-AP treatment. Accordingly, *in vivo* 4-AP treatment of EAEON appears to preserve myelin by non-immunological mechanisms, possibly by stabilization and/or protection of oligodendrocytes/myelin, or by enhancing remyelination and repair. We acknowledge that we cannot entirely rule out additional anti-inflammatory effects of

4-AP. The previous report on an attenuated Th1/Th17 polarization under 4-AP during $PLP_{139-151}$ induced EAE in SJL mice (Moriguchi *et al.*, 2018) as well as the trend towards less infiltration of CD3 positive lymphocytes in our optic nerve stainings could suggest additional anti-inflammatory mechanisms. However, this trend was not significant and all the data provided in our study, including the effects in the degenerative and toxic models, justify the conclusion that the predominant mode of action of 4-AP mediated protection in our experiments is not anti-inflammatory.

To elucidate the mode of action further, we moved to *in vitro* investigations using primary cell cultures and organotypic slice cultures. We acknowledge that the concentrations of ∼0.1–1 mM required for our *in vitro* investigations were approximately $100–1000\times$ higher than the concentration achieved *in vivo*. The targeted serum levels of 4-AP in patients with multiple sclerosis are ∼640 nM (van Diemen *et al.*, 1993), and the mean peak concentration in serum after oral intake of 25 mg immediate release 4-AP is ∼1 µM or 530 nM after intake of 20 mg of the sustained-release formulation (analytical specification form, U.S. National Medical Services, 2010). Notably however, the required concentrations depend on the extracellular milieu and the opening probability of ion channels. In most cell culture models, much higher concentrations of 4-AP are needed *in vitro* to affect K_v or calcium (Ca^{2+}) channels than in the serum of multiple sclerosis patients with tolerable doses. *In vitro*, the reported IC_{50} value of 4-AP is in the millimolar range for affecting K_v channels on dissociated neurons, dorsal root ganglia (Wu *et al.*, 2009), lymphocytes (Choquet and Korn, 1992), voltage-activated Ca^{2+} channels on dissociated neurons or dorsal root ganglia (Wu *et al.*, 2009) or acid gated ion channels on primary hippocampal neurons or Chinese hamster ovary cells (Vergo *et al.*, 2011).

Our *in vitro* experiments on cerebellar slice cultures indicate that prophylactic treatment also protects against toxic demyelination, supporting our *in vivo* data of preserved optic nerve myelin in EAEON.

Our primary cell culture experiments demonstrate that 4-AP, at nanomolar or micromolar concentrations, has no effect on the viability of axotomized RGCs *in vitro* and even has toxic effects at 1 mM. This finding suggests that the neuroprotective effects observed *in vivo* depend on the extracellular environment and may result from effects on surrounding cells rather than on RGCs themselves. As we observed preserved myelin in EAEON and the organotypic slice cultures, we investigated the effects of 4-AP on oligodendroglial cells *in vitro*, and indeed, prophylactic treatment with 1 mM 4-AP significantly protected mOPCs and rOPCs from glutamate toxicity. 4-AP treatment increased the cellular Ca^{2+} content and nuclear translocation of NFATc1 in OPCs. This result is unsurprising as 4-AP treatment reportedly increases cellular calcium levels, albeit in neuronal cells (Gibson and Manger, 1988; Tibbs *et al.*, 1989), and calcineurin-dependent nuclear translocation of NFAT proteins occurs with increasing levels of intracellular calcium (Hogan *et al.*, 2003). Interestingly, a recent publication reported an

important role for NFAT in OPC maturation and differentiation, suggesting that NFAT proteins interact with Sox10 to relieve repression of the transcription factors *Olig2* and *Nkx2.2*, leading to oligodendroglial differentiation and myelination (Weider *et al.*, 2018). However, 4-AP did not alter the differentiation of rOPCs *in vitro*, suggesting the involvement of additional distinctive mechanisms. Additional *in vivo* and *in vitro* investigations are already underway to elucidate the molecular basis of 4-AP's protective mode of action.

In summary, we provide compelling *in vivo* evidence that 4-AP, in addition to its well-known symptomatic effects, can modify the disease course of EAEON by preserving visual function, inner retinal layer thickness and myelin status. These data are supported by clinical data from a longitudinal retrospective study of patients with multiple sclerosis receiving symptomatic 4-AP therapy. Preliminary *in vitro* evidence suggests the involvement of cellular calcium levels and the NFAT pathway, but further investigations are warranted to elucidate the exact molecular mechanisms underlying 4-AP's neuroprotective effect.

Competing interests

M.D. received speaker honoraria from Novartis and Merck. P.G. performed consultancy work for GeNeuro and received support from the Research Commission of the medical faculty of the Heinrich Heine University. J.H. reports a grant for OCT research from the Friedrich-Baur-Stiftung; personal fees and nonfinancial support from Merck, Novartis, Roche, Bayer HealthCare, Santhera, Biogen, and Sanofi Genzyme; and nonfinancial support from the Guthy-Jackson Charitable Foundation and is (partially) funded by the German Federal Ministry of Education and Research under 01ZZ1603[A-D] and 01ZZ1804[A-H] (DIFUTURE). P.M. has received travel grants from Merck Sereno and Sanofi Genzyme. A.C.-H. received a Postdoctoral Fellowship from the National MS Society [by a Postdoctoral Fellowship from the National MS Society to Andrés Cruz-Herranz (FG-20102-A-1)]. S.Sa. has received consulting fees from Medical Logix for the development of CME programs in neurology and has served on scientific advisory boards for Biogen Idec, Genzyme, Genentech Corporation, EMD Serono and Novartis. He is the PI of investigator-initiated studies funded by Genentech Corporation and Biogen Idec and received support from the Race to Erase MS foundation. He has received equity compensation for consulting from JuneBrain LLC, a retinal imaging device developer. He is also the site investigator of a trial sponsored by MedDay Pharmaceuticals. A.U.B. is cofounder and shareholder of technology start-ups Nocturne GmbH and Motognosis GmbH. He is named on several patent applications describing serum biomarkers in multiple sclerosis, visual perceptive computing-based motion analysis and retinal image analysis. P.K. performed consultancy work for GeNeuro and received support from Sanofi Genzyme, French societies ARSEP and AFM, Deutsche Forschungsgemeinschaft (DFG; grants KU1934/2_1, KU1934/5-1), Stifterverband/Novartisstiftung and from James and Elisabeth Cloppenburg, Peek, and Cloppenburg Düsseldorf Stiftung. C.B. received research support from Biogen. O.A. received grants from the German Research Foundation (DFG) and the German Ministry of Education and Research (BMBF); grants and personal fees from Bayer HealthCare, Biogen, Genzyme, Novartis, and Teva; and personal fees from Almirall, MedImmune, Merck Serono, and Roche. P.A.C. has received consulting fees from Disarm Therapeutics and Biogen, and is PI on grants to JHU from Biogen and Annexon. H-P.H. has received fees for serving on steering committees from Biogen Idec, GeNeuro, Sanofi Genzyme, Merck, Novartis Pharmaceuticals, Octapharma, Opexa Therapeutics, Teva Pharmaceuticals, MedImmune, Bayer HealthCare, Forward Pharma, and Roche; fees for serving on advisory boards from Biogen Idec, Sanofi Genzyme, Merck, Novartis Pharmaceuticals, Octapharma, Opexa Therapeutics, Teva Pharmaceuticals, and Roche; and lecture fees from Biogen Idec, Sanofi Genzyme, Merck, Novartis Pharmaceuticals, Octapharma, Opexa Therapeutics, Teva Pharmaceuticals, MedImmune, and Roche. P.A. received compensation for serving on Scientific Advisory Boards for Ipsen, Novartis, and Biogen; he received speaker honoraria and travel support from Novartis, Teva, Biogen, Merz Pharmaceuticals, Ipsen, Allergan, Bayer HealthCare, Esai, UCB and Glaxo Smith Kline; he received research support from Novartis, Biogen, Teva, Merz Pharmaceuticals, Ipsen, and Roche. The MS Center at the Department of Neurology in Düsseldorf is supported in part by the Walter and Ilse Rose Foundation by grants to H-P.H. The other authors report no disclosures.

Supplementary material

Supplementary material is available at *Brain* online.

References

Albrecht P, Blasberg C, Ringelstein M, Muller A-K, Finis D, Guthoff R, et al. Optical coherence tomography for the diagnosis and monitoring of idiopathic intracranial hypertension. J Neurol 2017; 264: 1370–80.

Albrecht P, Muller A-K, Sudmeyer M, Ferrea S, Ringelstein M, Cohn E, et al. Optical coherence tomography in parkinsonian syndromes. PLoS One 2012; 7: e34891.

Balcer LJ, Balk LJ, Brandt AU, Calabresi PA, Martinez-Lapiscina EH, Nolan RC, et al. The International Multiple Sclerosis Visual System Consortium. Advancing visual system research in multiple sclerosis. J Neuroophthalmol 2018; 38: 494–501.

Bhargava P, Lang A, Al-Louzi O, Carass A, Prince J, Calabresi PA, et al. Applying an open-source segmentation algorithm to different OCT devices in multiple sclerosis patients and healthy controls. Implications for clinical trials. Mult Scler Int 2015; 2015: 136295.

Bostock H, Sears TA, Sherratt RM. The effects of 4-aminopyridine and tetraethylammonium ions on normal and demyelinated mammalian nerve fibres. J Physiol 1981; 313: 301–15.

Broicher SD, Filli L, Geisseler O, Germann N, Zorner B, Brugger P, et al. Positive effects of fampridine on cognition, fatigue and depression in patients with multiple sclerosis over 2 years. J Neurol 2018; 265: 1016–25.

Choi JW, Gardell SE, Herr DR, Rivera R, Lee C-W, Noguchi K, et al. FTY720 (fingolimod) efficacy in an animal model of multiple sclerosis requires astrocyte sphingosine 1-phosphate receptor 1 (S1P1) modulation. Proc Natl Acad Sci U S A 2011; 108: 751–6.

Choquet D, Korn H. Mechanism of 4-aminopyridine action on voltage-gated potassium channels in lymphocytes. J Gen Physiol 1992; 99: 217–40.

Cruz-Herranz A, Balk LJ, Oberwahrenbrock T, Saidha S, Martinez-Lapiscina EH, Lagreze WA, et al. The APOSTEL recommendations for reporting quantitative optical coherence tomography studies. Neurology 2016; 86: 2303–9.

Dietrich M, Cruz-Herranz A, Yiu H, Aktas O, Brandt AU, Hartung H-P, et al. Whole-body positional manipulators for ocular imaging of anaesthetised mice and rats. A do-it-yourself guide. BMJ Open Ophthalmol 2017; 1: e000008.

Dietrich M, Hecker C, Hilla A, Cruz-Herranz A, Hartung H-P, Fischer D, et al. Using optical coherence tomography and optokinetic response as structural and functional visual system readouts in mice and rats. J Vis Exp 2019; 143: e58571.

Dietrich M, Helling N, Hilla A, Heskamp A, Issberner A, Hildebrandt T, et al. Early alpha-lipoic acid therapy protects from degeneration of the inner retinal layers and vision loss in an experimental autoimmune encephalomyelitis-optic neuritis model. J Neuroinflamm 2018; 15: 71.

Gibson GE, Manger T. Changes in cytosolic free calcium with 1,2,3,4-tetrahydro-5-aminoacridine, 4-aminopyridine and 3,4-diaminopyridine. Biochem Pharmacol 1988; 37: 4191–6.

Gobel K, Wedell J-H, Herrmann AM, Wachsmuth L, Pankratz S, Bittner S, et al. 4-Aminopyridine ameliorates mobility but not disease course in an animal model of multiple sclerosis. Exp Neurol 2013; 248: 62–71.

Goodman AD, Bethoux F, Brown TR, Schapiro RT, Cohen R, Marinucci LN, et al. Long-term safety and efficacy of dalfampridine for walking impairment in patients with multiple sclerosis. Results of open-label extensions of two Phase 3 clinical trials. Mult Scler 2015; 21: 1322–31.

Goodman AD, Brown TR, Edwards KR, Krupp LB, Schapiro RT, Cohen R, et al. A phase 3 trial of extended release oral dalfampridine in multiple sclerosis. Ann Neurol 2010; 68: 494–502.

Goodman AD, Brown TR, Krupp LB, Schapiro RT, Schwid SR, Cohen R, et al. Sustained-release oral fampridine in multiple sclerosis: a randomised, double-blind, controlled trial. Lancet 2009; 373: 732–8.

Goodman AD, Cohen JA, Cross A, Vollmer T, Rizzo M, Cohen R, et al. Fampridine-SR in multiple sclerosis. A randomized, double-blind, placebo-controlled, dose-ranging study. Mult Scler 2007; 13: 357–68.

Gottle P, Kremer D, Jander S, Odemis V, Engele J, Hartung H-P, et al. Activation of CXCR7 receptor promotes oligodendroglial cell maturation. Ann Neurol 2010; 68: 915–24.

Grozdanov V, Muller A, Sengottuvel V, Leibinger M, Fischer D. A method for preparing primary retinal cell cultures for evaluating the neuroprotective and neuritogenic effect of factors on axotomized mature CNS neurons. Curr Protoc Neurosci 2010; 53: 3.22.1–.22.10.

Hogan PG, Chen L, Nardone J, Rao A. Transcriptional regulation by calcium, calcineurin, and NFAT. Genes Dev 2003; 17: 2205–32.

Horton L, Conger A, Conger D, Remington G, Frohman T, Frohman E, et al. Effect of 4-aminopyridine on vision in multiple sclerosis patients with optic neuropathy. Neurology 2013; 80: 1862–6.

Hupperts R, Lycke J, Short C, Gasperini C, McNeill M, Medori R, et al. Prolonged-release fampridine and walking and balance in MS. Randomised controlled MOBILE trial. Mult Scler 2016; 22: 212–21.

Jukkola P, Gu Y, Lovett-Racke AE, Gu C. Suppression of inflammatory demyelinaton and axon degeneration through inhibiting Kv3 channels. Front Mol Neurosci 2017; 10: 344.

Leibinger M, Muller A, Andreadaki A, Hauk TG, Kirsch M, Fischer D. Neuroprotective and axon growth-promoting effects following inflammatory stimulation on mature retinal ganglion cells in mice depend on ciliary neurotrophic factor and leukemia inhibitory factor. J Neurosci 2009; 29: 14334–41.

Lepka K, Volbracht K, Bill E, Schneider R, Rios N, Hildebrandt T, et al. Iron-sulfur glutaredoxin 2 protects oligodendrocytes against damage induced by nitric oxide release from activated microglia. Glia 2017; 65: 1521–34.

Leussink VI, Montalban X, Hartung H-P. Restoring axonal function with 4-aminopyridine. Clinical efficacy in multiple sclerosis and beyond. CNS Drugs 2018; 32: 637–51.

Mey J, Thanos S. Intravitreal injections of neurotrophic factors support the survival of axotomized retinal ganglion cells in adult rats in vivo. Brain Res 1993; 602: 304–17.

Moriguchi K, Miyamoto K, Fukumoto Y, Kusunoki S. 4-Aminopyridine ameliorates relapsing remitting experimental autoimmune encephalomyelitis in SJL/J mice. J Neuroimmunol 2018; 323: 131–5.

Morrow SA, Rosehart H, Johnson AM. The effect of Fampridine-SR on cognitive fatigue in a randomized double-blind crossover trial in patients with MS. Mult Scler Relat Disord 2017; 11: 4–9.

Pietroboni AM, Dell'Arti L, Caprioli M, Scarioni M, Carandini T, Arighi A, et al. The loss of macular ganglion cells begins from the early stages of disease and correlates with brain atrophy in multiple sclerosis patients. Mult Scler 2017; 25: 31–8.

Polman CH, Reingold SC, Banwell B, Clanet M, Cohen JA, Filippi M, et al. Diagnostic criteria for multiple sclerosis. 2010 revisions to the McDonald criteria. Ann Neurol 2011; 69: 292–302.

Prusky GT, Alam NM, Beekman S, Douglas RM. Rapid quantification of adult and developing mouse spatial vision using a virtual optomotor system. Invest Ophthalmol Vis Sci 2004; 45: 4611–6.

Reich DS, Lucchinetti CF, Calabresi PA. Multiple sclerosis. N Engl J Med 2018; 378: 169–80.

Rossi S, Lo Giudice T, V de C, Musella A, Studer V, Motta C, et al. Oral fingolimod rescues the functional deficits of synapses in experimental autoimmune encephalomyelitis. Br J Pharmacol 2012; 165: 861–9.

Schmalhofer WA, Bao J, McManus OB, Green B, Matyskiela M, Wunderler D, et al. Identification of a new class of inhibitors of the voltage-gated potassium channel, Kv1.3, with immunosuppressant properties. Biochemistry 2002; 41: 7781–94.

Stellmann J-P, Cetin H, Young KL, Hodecker S, Pottgen J, Bittersohl D, et al. Pattern of gray matter volumes related to retinal thickness and its association with cognitive function in relapsing-remitting MS. Brain Behav 2017; 7: e00614.

Tewarie P, Balk L, Costello F, Green A, Martin R, Schippling S, et al. The OSCAR-IB consensus criteria for retinal OCT quality assessment. PLoS One 2012; 7: e34823.

Tibbs GR, Barrie AP, van Mieghem FJ, McMahon HT, Nicholls DG. Repetitive action potentials in isolated nerve terminals in the presence of 4-aminopyridine. Effects on cytosolic free Ca2 + and glutamate release. J Neurochem 1989; 53: 1693–9.

Tseng K-C, Li H, Clark A, Sundem L, Zuscik M, Noble M, et al. 4-Aminopyridine promotes functional recovery and remyelination in acute peripheral nerve injury. EMBO Mol Med 2016; 8: 1409–20.

van Diemen HA, Polman CH, Koetsier JC, van Loenen AC, Nauta JJ, Bertelsmann FW. 4-Aminopyridine in patients with multiple sclerosis: dosage and serum level related to efficacy and safety. Clin Neuropharmacol 1993; 16: 195–204.

Vergo S, Craner MJ, Etzensperger R, Attfield K, Friese MA, Newcombe J, et al. Acid-sensing ion channel 1 is involved in both axonal injury and demyelination in multiple sclerosis and its animal model. Brain 2011; 134: 571–84.

Warner CV, Syc SB, Stankiewicz AM, Hiremath G, Farrell SK, Crainiceanu CM, et al. The impact of utilizing different optical coherence tomography devices for clinical purposes and in multiple sclerosis trials. PloS One 2011; 6: e22947.

Weider M, Starost LJ, Groll K, Kuspert M, Sock E, Wedel M, et al. Nfat/calcineurin signaling promotes oligodendrocyte differentiation and myelination by transcription factor network tuning. Nat Commun 2018; 9: 899.

Wu Z-Z, Li D-P, Chen S-R, Pan H-L. Aminopyridines potentiate synaptic and neuromuscular transmission by targeting the voltage-activated calcium channel beta subunit. J Biol Chem 2009; 284: 36453–61.